Production of Compacted Graphite Irons Through Two-Step Treatment Method

O. M. Suarez, Department of General Engineering, University of Puerto Rico-Mayagüez, Puerto Rico
C. R. Loper. Jr., Department of Materials Science and Engineering, University of Wisconsin-Madison, WI USA

Abstract

A study of compacted graphite iron production in a laboratory environment was conducted by carefully monitoring the chemical composition of the charge material, the thermal history of the melt and the addition of trimming alloys. The procedure, consisting of a two-stage process, was based on the reoxidation of a magnesium-treated melt by pouring the treatment ladle into the post-treatment furnace where the melt was reheated above 1400°C. An in-stream inoculation with 75% ferrosilicon inoculant was incorporated during final pouring. After final inoculation, the resulting microstructure was that of a compacted graphite iron with no carbide formation. The experimental process produced graphite with consistent compacted morphology without the use of titanium that could have been detrimental to tool life upon machining.

Riassunto

È stato condotto uno studio per la produzione di ghisa a grafite compatta in ambiente di laboratorio, monitorando accuratamente la composizione chimica del materiale di carica, la storia termica del liquido ed il dosaggio degli elementi d'aggiunta. Il procedimento, suddiviso in due stadi, si basa sulla riossidazione di una lega liquida, trattata con magnesio, mediante travaso del bagno in un forno di post-trattamento in cui il liquido viene riscaldato ad una temperatura superiore a 1400°C. Una inoculazione al 75% di ferrosilicio viene effettuata durante la colata finale. Dopo quest'ultima inoculazione la microstruttura è quella di una ghisa a grafite compatta esente da carburi. Il processo sperimentale impiegato consente perciò di ottenere grafite compatta senza utilizzare ittanio che potrebbe avere un effetto deleterio sull'utensile nel corso della lavorazione meccanica.

Introduction

The increasing demand of cast lightweight materials such as aluminum and metal-matrix composites in the automotive industry has propelled the production of new or more efficient techniques and manufacturing methods. Although much energy has been spent in developing those new lightweight alloys, cast iron has remained a competitive material due, in part, to its low production cost. In fact, one type of cast iron is an aggressive alternative to these lightweight alloys: compacted graphite iron (CGI). Nowadays, it is accepted that CGI can effectively reduce the total weight of an automobile by virtue of its high strength -when compared to other cast irons and aluminum alloys. In this case the use of the strength-to-density ratio gives CGI a clear advantage over other materials. Other characteristics make CGI a more attractive alternative such as: higher fatigue limit, higher yield stress, excellent machinability (depending on the production method), better modulus of elasticity, low thermal expansion, good thermal conductivity, and favorable casting properties.

Basics of CGI

Nonetheless, a universally accepted method of production that is suitable for commercial use in a high production volume is still to be developed. Several metallurgical variables need to be strictly controlled in order to achieve consistent CGI properties in a production line at reasonable costs. This situation has hindered the application of this material in, for instance, automotive parts.

More recently a few alternative processing have been worked out gradually and then patented [1,2]. The process-control thermal analysis appears to implement a relatively dependable method based on thermal analysis, process modeling, and melt chemistry adjustments through a modular set up. Severe limitations of these CGI production methods include: lack of versatility that limits their applicability to different carbon equivalent (CE) ranges; lack of transparent assessment and treatment of measured variable values that compromise on-line corrections by trained operators; disregard of important foundry variables in the model assessment; and high cost of sampling procedures.

Therefore, the present research intends to provide the basis of an alternative method for the

on-line control of CGI melts where the iron is adequately characterized in order to ensure reliability and repeatability of the process while the entire control instrumentation is both robust and inexpensive.

Adequately produced CGI consist of a microstructure containing mostly worm or vermicular shaped graphite particles that are about 50 μm long with typical aspect ratios of less than 10. In other words. graphite particles should be mostly of type IV as defined by the ASTM A 247 Standard. Gan and Loper [3] indicated that CG morphology is not determined by the nucleation characteristics but by the local growth conditions imposed by solidification variables. In general it can be stated that interconnectivity of CG is circumscribed to local regions. This particularity gives CGI an intermediate behavior between gray and ductile irons.

Although the existence of compacted graphite irons has been known for many years [4], only in the last decades were they applied to more specific machinery components. This considerable attention was due to the properties of CG irons that allow this material to fill the property gap left between gray and ductile irons.

As mentioned, a major limitation in the production of CG irons is the requirement of a strict process control. The spheroidization of graphite in cast irons via small amounts of nodulizing elements (Mg, Ce and other rare earths) to the melt promotes a structural change in the formation of graphite. A vermicular microstructure results when the nodularization treatment is insufficient to form spheroidal graphite although the vermicular structure develops exclusively during eutectic solidification. In fact, as in the case of modified eutectic silicon in Al-Si alloys, this vermicular graphite is an interconnected, fibrous phase [5]. For this reason it is often said that CGI physical properties are closer to gray irons than to ductile irons [6]. Good machinability and better thermal conductivity as well as less secondary shrinkage tendency than in nodular irons, led to the use of CGI for thick section castings. Vermicular graphite is difficult to extract during machining, therefore, surface crevices that can act as corrosion cells are not common in CGI parts. CG irons have been used in truck engine manifolds where gray irons fail by thermal fatigue and nodular irons experience severe heat distortion [7]. In table I nominal mechanical properties for different CG irons are displayed as obtained for 30.5 mm test bars by Aleksandrov *et al* [8]. Independently from the pearlite-to-ferrite ratio present in the microstructure, usual longitudinal elastic moduli are close to 144 GPa [4]. In addition, Aleksandrov reported that statistical tests proved that as-cast mechanical properties are mostly determined by the carbon and manganese contents.

Fatigue limits on the order of 153 MPa (pearlitic matrix) and 118.6 MPa (ferritic matrix) are slightly higher than fatigue strengths in gray irons [8]. Reported relative damping capacities of CGI, gray irons and ductile irons are: 0.6, 1.0, and 0.34 [9]. Additionally, it has been indicated that thermal conductivity is comparable to that of gray iron and much higher than that of nodular iron [10]. The combination of all these features make CGI a more suitable material for high performance internal combustion engine blocks where high temperature strength, vibration damping, and appropriate heat extraction conditions are prevalent requirements.

Commercial and Experimental CGI Production

As indicated previously, a great limitation in the application of CG irons is the need for exacting graphite morphology control upon processing. General specifications tolerate at most 10-20% of nodular graphite particles with no flake graphite in commercial CG irons [6]. Cornell and Loper [11] provided a detailed analysis for section sizes from 12.7-127 mm. In addition to carbon and silicon, magnesium content should be monitored conscientiously since residual Mg contents out of the 0.005% - 0.008% range could result in an excessively flake microstructure for the lower Mg values or in an exceedingly nodular one, for higher Mg levels. In this case, the use of lanthanides combined with magnesium can compensate the deficiency in graphite morphology [11] as well as to provide resistance to fading of the structure to flake graphite.

Several methods have been experimentally implemented to produce CGI. For instance, as reported by Monroe and Bates [12], it is possible to desulfurize the base metal to attain very low values of sulfur and then allow for a rapid solidification. The addition of controlled amounts of spheroidizing elements such as Mg or Ce can also be used. Finally, treating the molten metal with both spheroidizing and anti-spheroidizing elements, mainly Ti, at the same time can provide optimum results in many applications.

Indeed, the Ti process appears to be a reliable CGI production method with repetitive results. However, one important factor impedes the general application of this treatment: titanium has a strong carbide, and nitrocarbide formation tendency. TiC and complex Ti nitrocarbides are very hard phases that diminish machining tool lifetime. Whenever possible such phases should be avoided in CGI parts where exacting or heavy machining processes are required.

Nofal *et al* compiled all possible alternatives for the production of compacted graphite [13]. From this categorizing it becomes apparent that most of alternatives deal somehow with the addition of nodulazing agents such as magnesium, cerium and rare earths (RE).

TWO-STEP LABORATORY PRODUCTION OF CGI

The main objective of this experimental part was to study alternative methods for the preparation of CG irons. For this purpose a 45 Kg medium frequency coreless induction furnace was used. A number of preliminary experiments comprising different chemical compositions of the melt and operation settings were carried out and the general effect of molten iron handling on the resulting microstructure was assessed by microstructural analysis. Special consideration was given to the thermal history of each melt during melting, alloy addition for base iron production, nodulization (magnesium treatment) and final ferrosilicon inoculation. Also, the evolution of the molten metal chemical composition was followed by convenient sample extractions at predetermined times from the melt. Hence, alloying element losses can be estimated upon each step of the procedure and subsequently accounted for and corrected for the next heat. The reported heats are a sample of the several experiments conducted to fine-tune the procedure.

Table 1. Nominal mechanical properties for different CG irons

CGI Mechanical Properties				
% Pearlite	Brinnel Hardness	Min. Tensile Strength [MPa]	Min. Yield Stress (0.2% offset) [MPa]	Min. Elongation
90% Min.	217-270	448	379	1%
10-90%	163-241	345	276	1%
10% Max.	130-179	276	193	3-5%

MATERIALS AND EXPERIMENTAL PROCEDURES

In table 2 the chemical composition of the charge material, nodulazing alloy and inoculant as used in this investigation is shown. In order to eliminate the influence of charge material, the same material was used in different proportions according to the required chemical composition. It can be seen that base iron was produced with pig iron, cast iron returns, steel scrap, graphite as carbon raiser and high purity Fe-50%Si alloy as silicon raiser.

Table 2. Chemical composition of the charge material used in the CGI study

Material	%C	%Si	%P	%Mn	%S	%Mg	%Al	%Ca	%ti	%Cr	%Cu	%La	%Ce	%RE
Pig Iron	4.296	0.187	0.014	0.004	0.006									
Returns	3.77	2.33	0.0326	0.32	0.01					0.051	0.19			
Steel	0.71	0.13	0.02	0.245	0.007		0.069			0.032				
C Raiser	100													
Si Raiser		47.74					0.08	0.01	0.03					
MgFeSi		45.62				6.18	0.75	1.01		0.11		0.17	0.38	0.76
Inoculant		78.4					1.15	0.94						

TEMPERATURE CONTROL AND MELT PREPARATION

For these sets of experiments a double-step procedure was employed. Preliminary tests proved that this procedure was very dependable in terms of results and easiness of operating conditions and sampling techniques as discussed later. After complete melting, the molten metal temperature is recorded with a type-S lance while ramping up to the 1427°C-1466°C temperature range. Simultaneously at every step, thermal analysis samples were taken to determine the austenite liquidus and the carbide eutectic temperatures. TAW and TEW, respectively, obtained in tellurium-coated thermal analysis cartridges. These solidification parameters allowed adjusting the level of carbon in the melt according to previously obtained regression equations [14]. Tellurium-coated small thermocouple cups are utilized to determine those thermal parameters. Pertinent adjustments of carbon content in the melt with the addition of graphite follow accordingly. Once the required level of C is reached (according to the specifications of the given experiment), the melt is heated rapidly to about 1520°C-1538°C to attain the required superheat for Mg treatment. The maximum temperature is not held over 1540°F to minimize silicon loss, carbon burn-off and melt oxidation.

At the highest attained temperature, the furnace is shut off and sampling for chemical composition and thermal analyses proceeds. The acquired samples are identified as Base Iron for the purpose of subsequent data analysis. Melt temperature readings are taken successively until the temperature

reaches 1500°C. Treatments were conducted using an experimental tilting ladle that is indicated in the schematic of the entire two-stage procedure presented in fig. 1.

A 6%MgFeSi treating alloy covered with 500 g of clean scrap steel are placed on the bottom of the ladle and the base iron melt is poured into the preheated ladle. After removal of the slag resulting from the treatment, chemical composition and thermal analysis samples are obtained and identified as Treated Iron. Temperature measurements of the melt should indicate ~1400°C before reladling the molten iron back into the furnace.

After reladling, another sampling for chemical composition and thermal analysis is made. The corresponding samples are labeled as Reladled Iron. Presently, the furnace is ramped up to 1466°F for final inoculation and pouring into the molds. Inoculant FeSi at 0.55% of the melt weight is added in-stream while pouring into the preheated ladle where a 75 mm heel of molten metal should be present prior to the beginning of inoculation. After about 30 seconds, the latest temperature measurement is recorded and samples are obtained for thermal analysis and chemical composition. These post-inoculated specimens are labeled as Final Iron. Subsequently, the remaining material is poured into the molds.

ANALYSIS OF THE RESULTS

For a preliminary test of the double-step procedure the target CE and general chemical composition for the final irons shown in table 3 were selected and produced in Heat A. In fig. 2 the temperature profile upon processing is shown. This chart has proven to be extremely helpful in adjusting the general scheme for ensuing experimental heats. The different events during the entire process were labeled at the corresponding times. The initial data point in the chart was obtained right after the last added charge material melted down and before powering up the furnace.

The resulting microstructures can be seen in fig. 3 where photomicrographs at four different stages of the iron preparation are shown. These photographs were obtained at 100x magnification without etching the samples to distinctly display the graphite morphology at every stage. While the base iron contains lamellar graphite eutectic cells, after Mg treatment a complete nodular microstructure is produced. This is evident from the chemical analysis presented in table 3 where a Mg content of 0.0365%o accounted for such nodularity. Although in this and following preliminary experiments the addition of Ti was not considered, chemical analysis revealed that there was

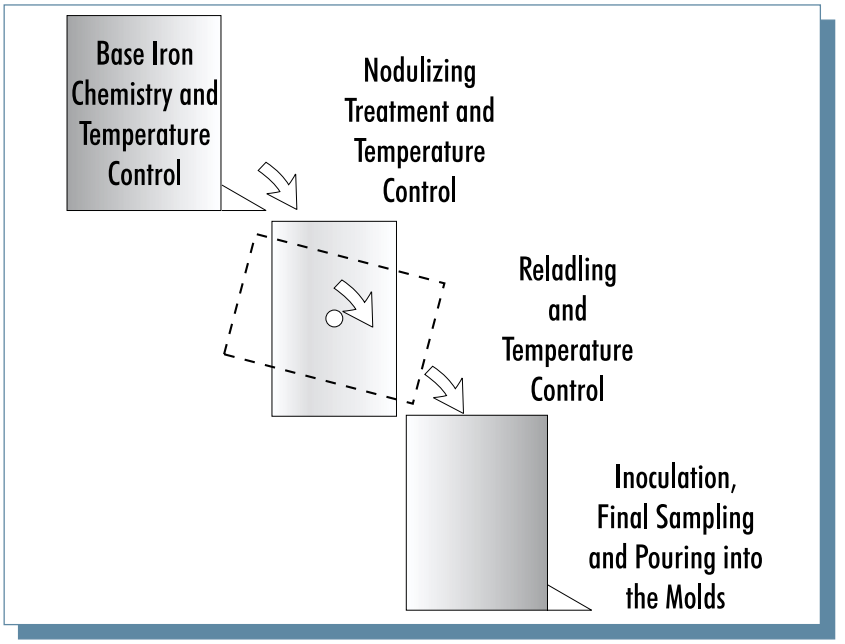

Fig. 1: Schematic of the experimental processing of compacted graphite iron melts

TABLE 3. SUMMARY OF CHEMICAL ANALYSIS OBTAINED FROM DIFFERENT MELT STAGES IN HEAT A

Heat A Chemistry Summary				
Iron	C.E.	C	Si	Mg
Base	4.155	3.845	0.93	0.0000
Treated	4.178	3.71	1.405	0.0365
Reladled	4.04	3.56	1.44	0.012
Final	4.18	3.49	2.07	0.008

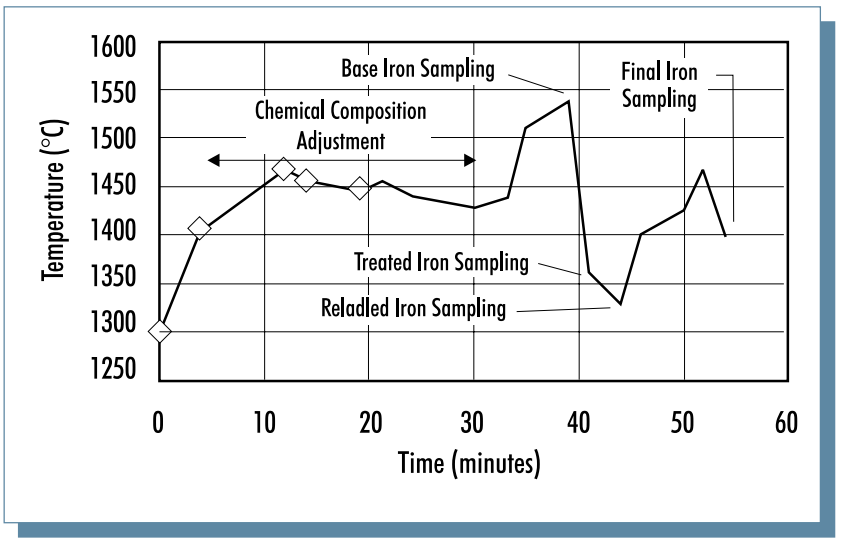

Fig. 2: Thermal history of the iron melt during Heat A

0.002 wt.% of Ti present in this Mg treated iron. Oxygen activity levels in the reladled iron climbs to around 0.000028 during the operation. After reladling due to such heavy oxidation generated in the melt by the turbulence upon processing, a mostly white microstructure originates as can be seen in the corresponding micrograph. At this stage the iron contains one third of the residual Mg upon treatment. Seemingly, this should be the preferred starting melt condition for a final vermicular microstructure just before inoculation with ferrosilicon. The assessed final Mg percentage was 0.008 wt.%. On the other hand the final target CE of 4.18% was attained.

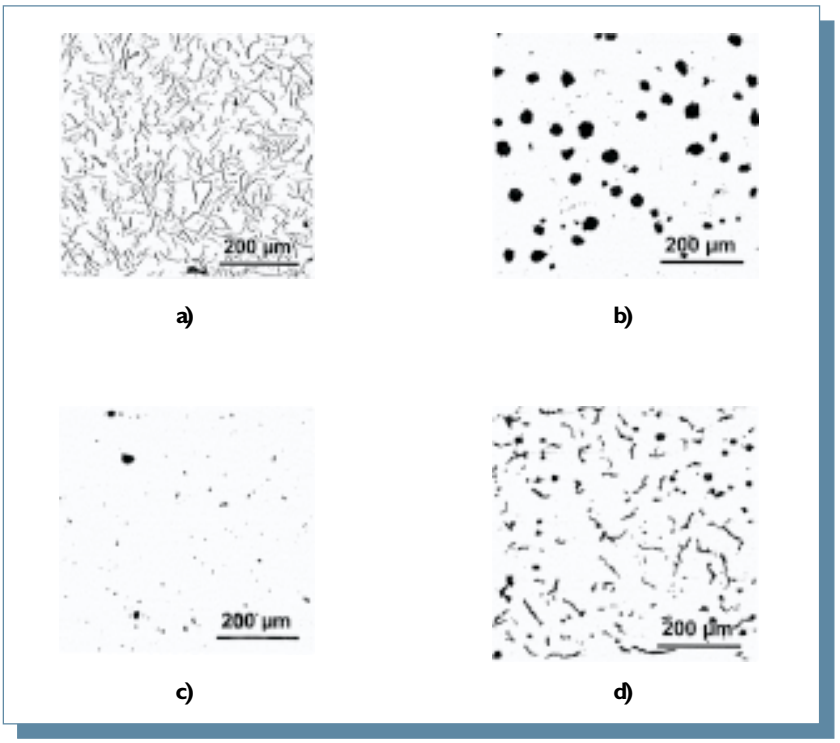

Fig. 3: Photomicrographs of the iron produced in Heat A at different processing stages. (unetched eìsamples). a) Base iron; b) Mg-Treated Iron; c) Reladled Iron; d) Final Iron

In a subsequent experiment (Heat B), the carbon level was slightly increased by 0,05% while silicon level was reduced by an equivalent amount. By this means, the previously selected CE value was preserved. The final magnesium level was also maintained. In table 4 the chemical composition of the four processed irons is shown.

The processing temperatures are indicated in the graph of fig. 4. The resulting microstructures at different processing stages are displaved in fig. 5 as obtained by metallographic preparation of the thermal analysis cups. While the reladled iron microstructure ends up as a mostly white with few graphite vermicules and nodules, the final microstructure reveals a dense mixture of vermicular and nodular graphite.

For the next experiment (Heat C) the same CE value was retained whereas carbon and silicon levels were about the same as in previous experiments, being only a small increase in final silicon. This resulted from increasing the amount of Mg-treating alloy so as to achieve a final residual magnesium of 0.013%. The process follow-up tempera-

Table 4. Summary of chemical analysis obtained from different melt stages in Heat B

Heat B Chemistry Summary				
Iron	C.E.	C	Si	Mg
Base	4.172	3.805	1.1	0.001
Treated	4.25	3.71	1.61	0.039
Reladled	4.21	3.68	1.6	0.011
Final	4.2	3.55	1.95	0.0085

Table 5. Summary of chemical analysis obtained from different melt stages in Heat C

Heat C Chemistry Summary				
Iron	C.E.	C	Si	Mg
Base	4.07	3.77	0.89	0.0005
Treated	4.183	3.715	1.405	0.039
Reladled	4.11	3.64	1.42	0.016
Final	4.275	3.525	2.25	0.013

Table 7. Mean thermal analysis parameters measured for heat A

Heat A Thermal Analysis Parameters in °C					
Sample	TAW	TEW	TAL	TEU	TER
Base Iron	1157.4	1130.5	1160.0	1131.7	1137.1
Treated Iron			1173.8	1137.9	1143.7
Reladled Iron			1182.0	1127.1	1130.2
Final Iron	1178.4	1123.8	1167.9	1146.3	1147.6

Table 7. Mean thermal analysis parameters measured for heat B

Heat B Thermal Analysis Parameters in °C					
Sample	TAW	TEW	TAL	TEU	TER
Base Iron	1155.4	1128.6	1159.1	1134.7	1144.5
Treated Iron			1166.8	11.35.1	1140.2
Reladled Iron			1171.3	1123.0	1124.2
Final Iron	1181.0	1129.0	1174.2	1153.0	1155.3

ture chart is given in fig. 6. In table 5 the corresponding chemistries are presented while the microstructural features are visible in fig. 7. Once again while oxygen activity raises (measured at 0.000024), a mostly white iron resulted after reladling the molten iron. After inoculation the attained microstructure is clearly vermicular. The slightly higher titanium (not shown in the chemistry tables), 0.013%, seems not to produce a significant effect on the vermicular graphite formation.

Further microstructural analysis performed in all final iron samples revealed the lack of carbides. Several other heats were completed in order to calibrate the process in terms of general operation and recovery adjustments for charge calculations [15] and corroborated the reported results. In all cases the oxygen activity measured consistently fall within the 0.000022-0.000034 range in the reladled irons.

Thermal Analysis Experiments

As indicated previously, at every process step the iron was sampled for chemical and thermal analyses. Small thermal analysis cartridges were employed to collect the whole set of cooling curves. The analog data was digitized by means of data acquisition board working at 2 Hz sampling rate. The data files were store in ASCII format by using commercial data acquisition software. Later the data were analyzed by using proprietary curve analysis software.

Two different types of thermocouple cups were used. A tellurium-coated one was employed to collect cooling curves from white irons in order to measure TAW and TEW while a non-tellurium coated served as a sensor for austenite liquidus TAL, eutectic undercooling TEU, and eutectic recalescence TER temperatures.

In table 6, the thermal parameters assessed during Heat A are indicated. In the case of Mg-treated and reladled irons non Te-coated cup was used. This was also the case in Heat B (table 7) and Heat C (table 8). Cooling curves in the ensuing cups were acquired at $4s^{-1}$. These preliminary tests were designed and completed in order to test the workability of the general two-step procedure set-up. Therefore they were not originally intended to provide intensive statistical basis for the examining in detail the thermal analysis data. Further experimentation is being conducted to establish an adequate correlation between those thermal analysis parameters and the microstructural features observed.

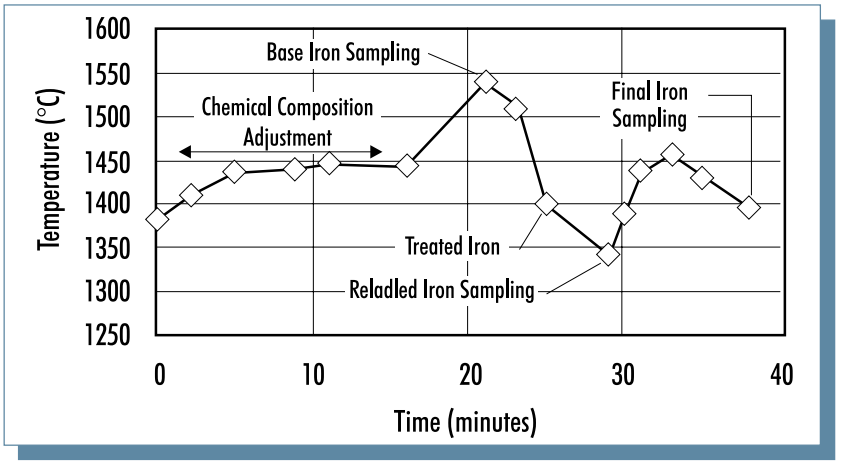

Fig. 4: Thermal history of the iron melt during Heat B

Table 7. Mean thermal analysis parameters measured for heat C

Heat C Thermal Analysis Parameters in °C					
Sample	TAW	TEW	TAL	TEU	TER
Base Iron	1167.7	1131.0	1171.0	1131.6	1136.5
Treated Iron			1172.6	1138.1	1140.9
Reladled Iron			1176.2	n/a	1125.1
Final Iron	1169.9	1163.4	1168.3	1152.3	1156.8

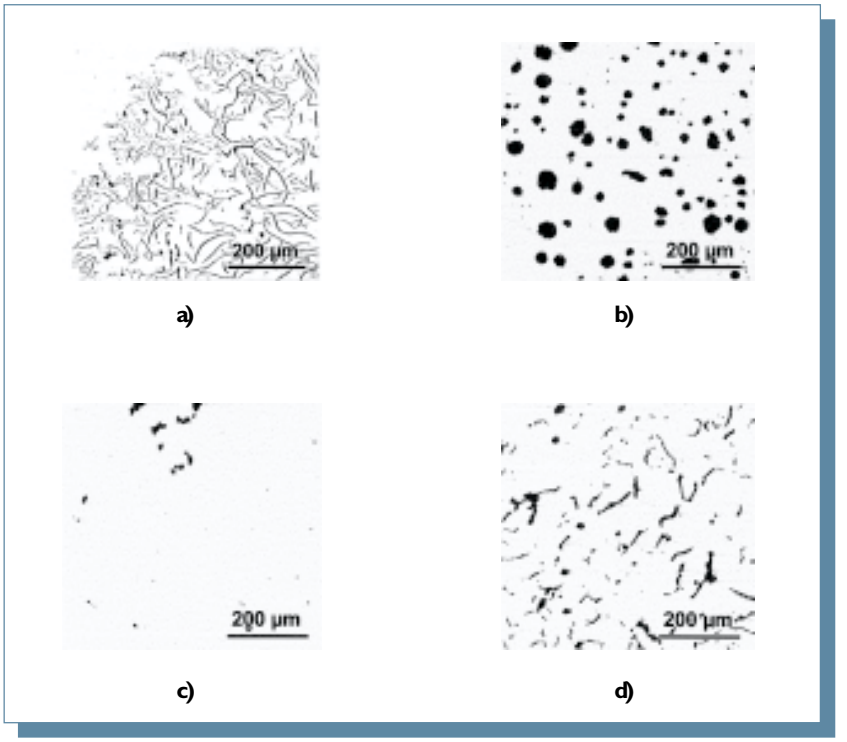

Fig. 5: Photomicrographs of the iron produced in Heat B at different processing stages. (unetched eisamples). a) Base iron; b) Mg-Treated Iron; c) Reladled Iron; d) Final Iron

CONCLUSIONS

In summarizing this investigation, it is clear that in order to produce an adequate vermicular microstructure by: this two-step procedure it is necessary to secure a mostly white microstructure upon reladling and reheating. In this procedure, however, a lamellar structure was absent in Heat B and C with similar Mg content. Two factors present in the experiments could have caused the appearance of flake graphite: a low CE value and a high post-inoculating silicon presence. In addition, temperature control is difficult when the melt is reladled and heavy losses due to oxidation are somewhat difficult to predict and then taken into account when computing recoveries for the following heat.

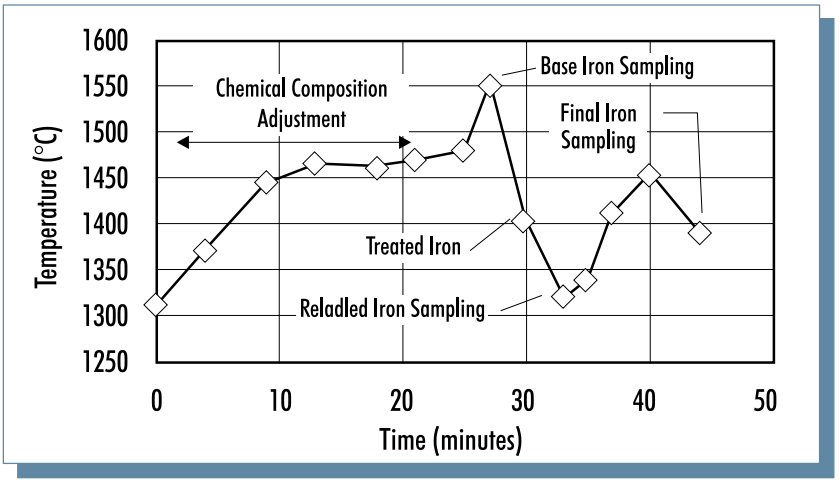

Fig. 6: Thermal history of the iron melt during Heat C

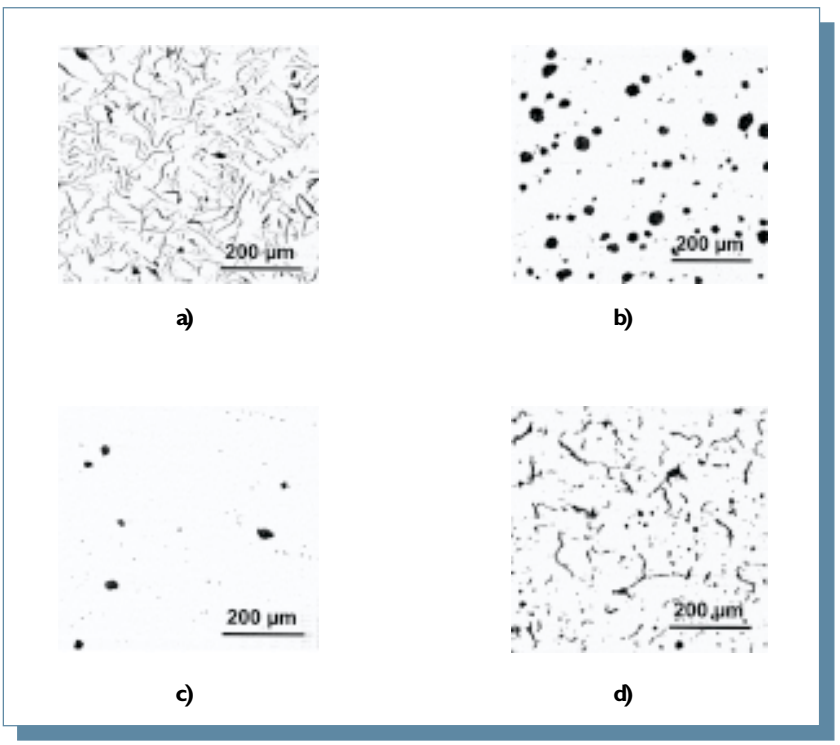

Fig. 7: Photomicrographs of the iron produced in Heat A at different processing stages. (unetched samples). a) Base Iron; b) Mg-Treated Iron; c) Reladled Iron; d) Final Iron

However, all those detrimental factors did not have any significance in the final occurrence of a CG structure. In essence, the main attainment of this experimentation has been to provide a strong basis for understanding the behavior of undertreated melt, i.e. with reduced modification (simulated by the heavy oxidation upon reladling), and proper inoculation.

Again it must be underscored that when low residual Mg is present due to insufficient MgFeSi alloy additions, isolated flake patches should be observed in CG microstructure. This effect was not noticed in any of the final irons produced through the two-step processing. Despite the turbulence and subsequent melt oxidation upon reladling, graphite morphology in the final iron microstructures shown in figs. 3, 5 and 7 is not significantly different. This result correlates properly with the consistent and recurring levels of oxygen activities found in the reladled (re-oxidized) irons. Furthermore, the final residual magnesium levels achieved in all CG irons varied from 0.008 to 0.013 wt. % Mg. This is within the low end of the residual Mg range in normal pearlitic CGI [2]. However, there is a notable differentiation in the proposed two-stage process: the levels of titanium in all base irons were below detection threshold. In other words, the resulting CG irons are free of deleterious TiC particles that would compromise the machinability of the materials. Additionally, the levels of Ce and rare earths (RE) in the Mg-treating alloy (0. 38 wt.% and 0. 76 wt.%, respectively) had a minor contribution to the general process.

Consequently, the proposed laboratory preparation of CGI bears some important advantageous features, as follows:

- No titanium addition was necessary.
- The Mg treating alloy used is a common, low Ce and RE- containing commercial alloy.
- The inoculant added was a low-cost commercial inoculant used in the production of ductile irons.
- Despite the seeming complexity of the process, the results are consistent and repetitive.

Moreover, this investigation clearly proves the importance of inoculation in the production of CGI as can be observed in the microstructural changes between reladled irons (before inoculation) and final post-inoculated CGI. It is believed that the effect of the inoculant is not to provide nucleating sites for CG since the procedure merely increases nodularity (an effect that is typically undesirable in CGI production) but to increase Si level in the melt to promote graphitization. This is so effectively achieved that no carbides formed

during solidification were observed in almost all analyzed microstructures. In closing, although this investigation was semiquantitative in nature, it provided sound information on the ability to produce CGI in a laboratory environment that can be implemented in a production line without major economic investment.

REFERENCES

1. Subramanian, S. V., Ghosh, D. S., Purdy, G. R., Kay, D. A. R., and Gray, J. M. Process for the production of vermicular cast iron. U.S. Patent N° 4227924, (1980).
2. SinterCast, Method for the Production of Compacted Graphite Cast Iron. Patent N° 5337799, (1994).
3. Gan, Y. and Loper Jr., C. R. Observations on the Formation of Graphite in Compacted and Spheroidal Graphite Cast Irons. *AFS Trans., 91,* (1983), 781-788.
4. Evans. E. R., Dawson, J.V., and Lalich, M. J. Compacted graphite cast irons and their production by a single alloy addition. *AFS Internotional Cast Mefals Research J. l.* (1976), 13-18.
5. Liu, P. C., Loper Jr., C. R., Kimura. T., and Pan. E. N. Observations on the graphite morphology of compacted graphite cast iron. *AFS Tmns,, 89.* (1981), 65-78.
6. Elliott, R. *Cast Iron Technology,* Butterworths & Co. Ltd.,London, (1988), pp. 20-22.
7. Chen, M., and Wan, R. *6th International Pacific Conference on Automotive Engineering,* Korean Society of Automotive Engineers, Seoul, South Korea, (1991): pp. 713.
8. Aleksandrov, N. N., Milman, B. S., Il'icheva, L.V., Osada, N. G., and Andreev, V. V. Production and Properties of High-Duty Iron with Compacted Graphite. *Russian Castings Production,* (1976), 319-322.
9. C. F. Walton and T. J. Opar, (Ed.), *Iron Castings Handbook,* Iron Castings Soc. Inc. (1981), pp. 381-397.
10. Stefanescu, D. M.. Hummer. R., and Nechtelberger, E. Compacted graphite irons. In *Metals Handbook Casting.* ASM International, Materials Park, Ohio. (1988), vol. 15, pp. 667-677.
11. Cornell, H. H., and Loper Jr., C. R. Variables Involved in the Production of Compacted Graphite Cast Iron Using Rare Earth-Containing Alloys. *AFS Trans., 93,* (1985), 435-442.
12, Monroe, R, W., and Bates, C. E. In P. K. Mikelonis (Ed.), *Foundry Technology: Source Book.* American Society for Metals, Materials Park. Ohio, (1982): pp. 268-291,
13. Nofal, A.A., Parent-Simonin, S., and Rezk, A. S. Contribution a 1'etude de la solidification de la fonte a graphite vermiculaire. *Fonderie-Fondeur d'Aujourd'hui.,83,* (1989), 14-24.
14. Suarez, O. M. and Loper Jr., C. R. Influence of Thermal Analysis Cup on the Assessment of Critical Temperatures upon Solidification of Cast Iron. *AFS Trans, 105,* (1997), 929-937.
15, Suarez, O. M. Thermal Analysis and Microstructure Control of Cast Irons. *Ph D Thesis.* University of Wisconsin – Madison, (2000).
16. Liu. J., Ding. N. X., Mercer, J. L, and Wallace, J. F. Effect of type and amount of treatment alloy on compacted graphite produced by the Flotret process. *AFS Trans., 93,* (1985), 675-688.